Supporting Information

S.1 Synthesis of Oligonucleotides

Oligonucleotides (ON1-ON6, Tab. 1) were synthesized at the 1.0 μmol scale using an automated DNA synthesizer. Standard cycle procedures were applied for unmodified phosphoramidites using 0.45 M solution of 1*H*-tetrazole as activator. Stepwise coupling yields, as determined by a spectrophotometric DMT+ assay were > 99% for standard phosphoramidites, > 95% for LNA amidites (15 min coupling time), and > 80% for incorporation of terpy-UNA (15 min coupling time). DMT+ was collected after deblocking, and absorbance at 495 nm was measured and compared to that of the following step.

The final step for the synthesis of ONs containing a 5´-C6-SH modification (ON1-ON4, Tab. 1) was the coupling of thiol-modifier C6 S-S (Glen Research, Virginia, USA), using 0.45 M solution of 1*H*-tetrazole as activator and 15 min coupling time. Removal of the nucleobase protecting groups and cleavage from solid support was effected using standard conditions (32% aqueous ammonia for 12 h at 55 ^{o}C).

All ONs were purified by DMT-ON RP-HPLC using a C18-column (10 μm, 300 mm × 7.8 mm) and the following eluent system: eluent-A, 95% 0.1 M Et_3N, 5% CH_3CN; eluent-B, 25% 0.1 M $Et_3NH{\cdot}HCO_3$, 75% CH_3CN; gradient, 0-5 min isocratic hold of 100% eluent-A, followed by a linear gradient to 55% eluent-B over 75 min at a flow rate of 1.0 mL/min.

Fractions containing pure ONs were collected and evaporated on speed-vac. ONs comprising a 5´-C6-SH modification were treated with dithiothreitol (100 mM, 100 μL, adjusted to pH 8.3-8.5 using triethylamine) for 30 min, followed by precipitation (anhydrous acetone, 1000 μL, -18 ^{o}C, 12 h) and washing with anhydrous acetone (3×1000 μL). For ONs without 5´-C6-SH modification, evaporation was followed by detritylation (80% aq. AcOH, 20 min), precipitation (anhydrous acetone, 1000 μL, -18 ^{o}C, 12 h) and washing with anhydrous acetone (3×1000 μL).

All ONs were finally desalted using commercially available NAP^{TM}-10 columns (GE Healthcare, Buckinghamshire, UK). Their composition and purity were verified by MALDI-MS analysis and ion-exchange HPLC (100 mm × 4.6 mm column size), respectively. The following eluent system was used: eluent-A, 25 mM Tris-Cl, 1 mM EDTA (pH 8.0); eluent-B, 1 M NaCl, gradient, 0-5 min isocratic hold of 95% eluent-A followed by a linear gradient to 70% eluent-B over 41 min at a flow rate of 0.75 mL/min. MALDI spectra are shown in Figs. S1-S6.

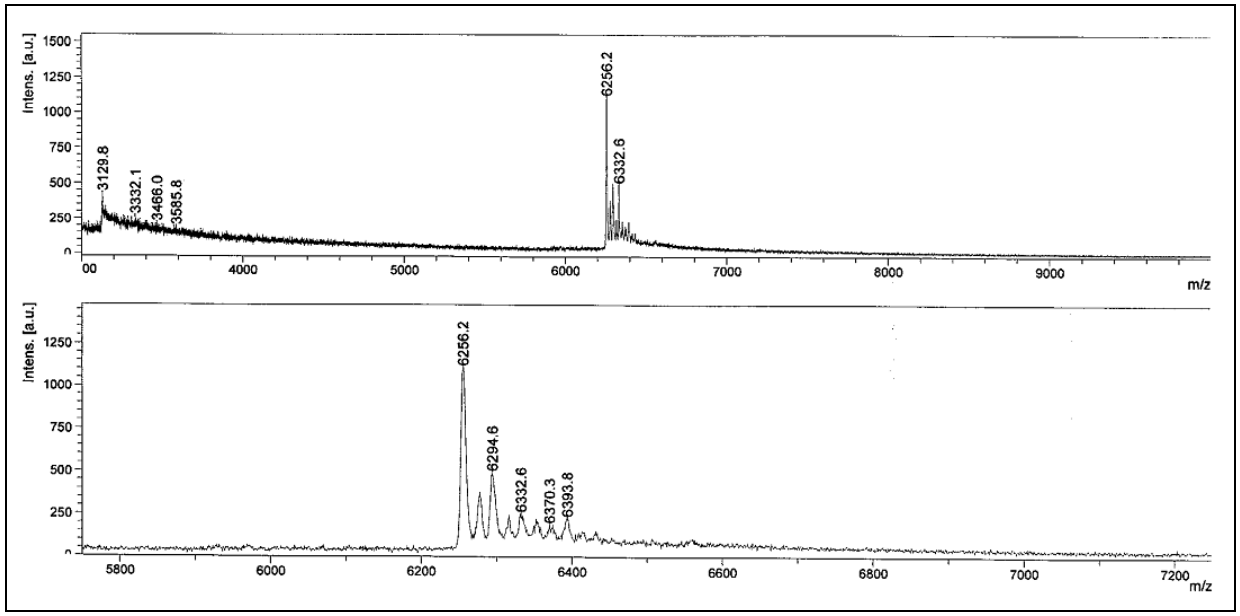

Fig. S1. MALDI-MS spectra of ON1 (5´-HS-C6-d(CGCATTATTACGC)).

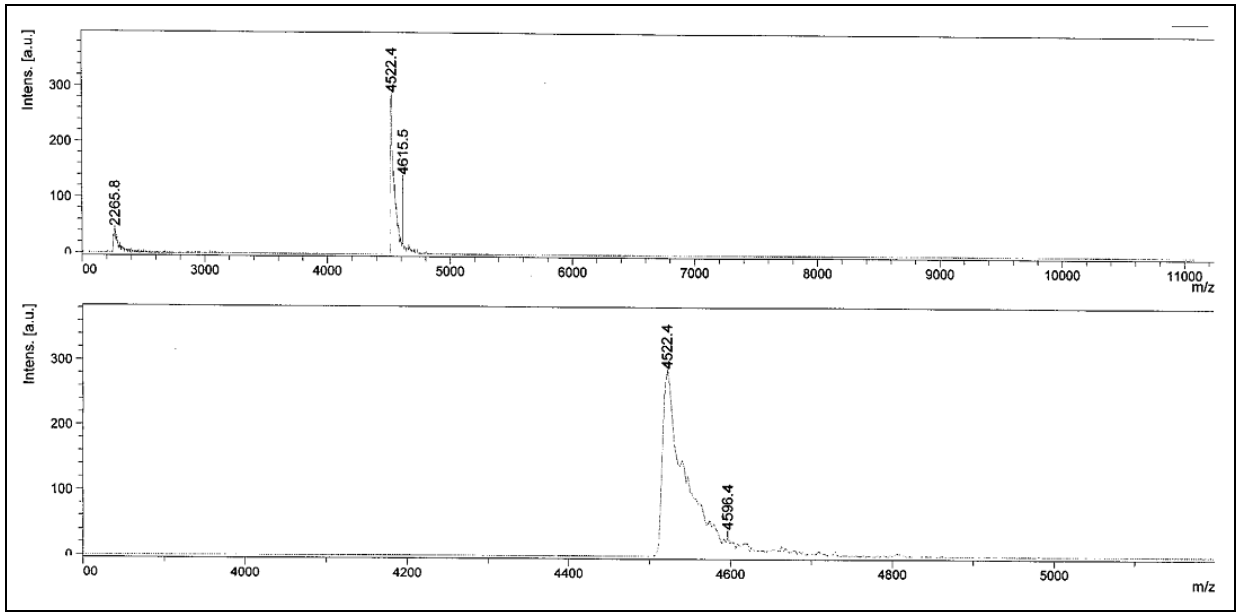

Fig. S2. MALDI-MS spectra of ON2 (5´-HS-C6-d(CGCAT**X**ATTACGC))

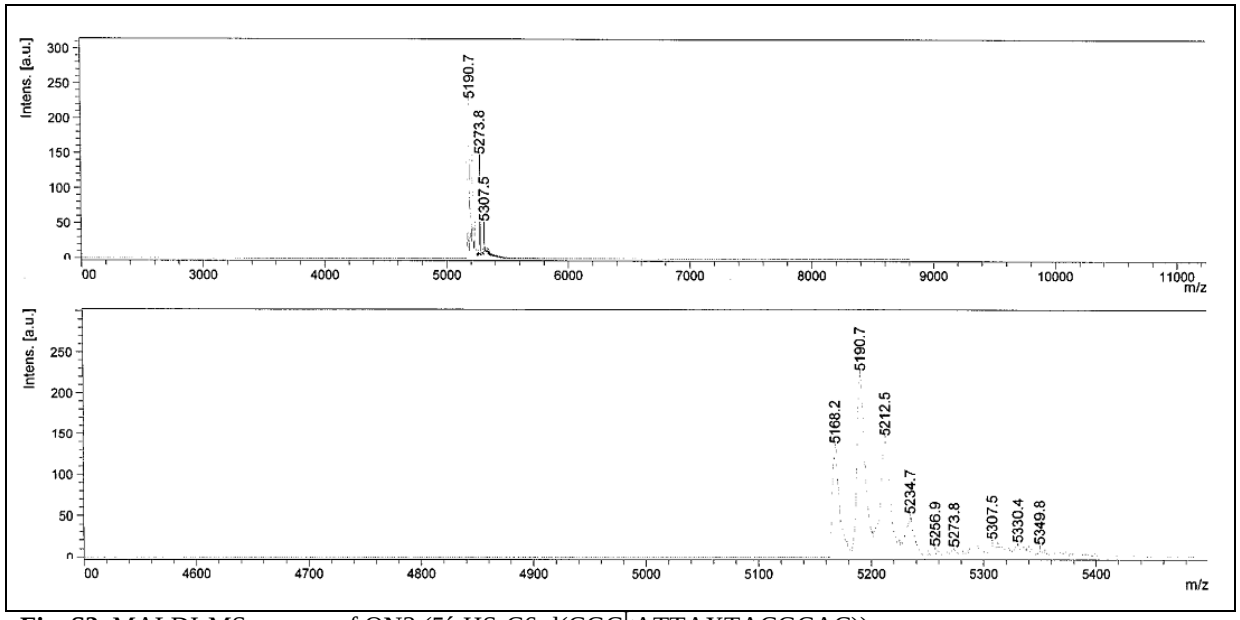

Fig. S3. MALDI-MS spectra of ON3 (5´-HS-C6-d(CGC^{L}ATTAXTACGCAC)).

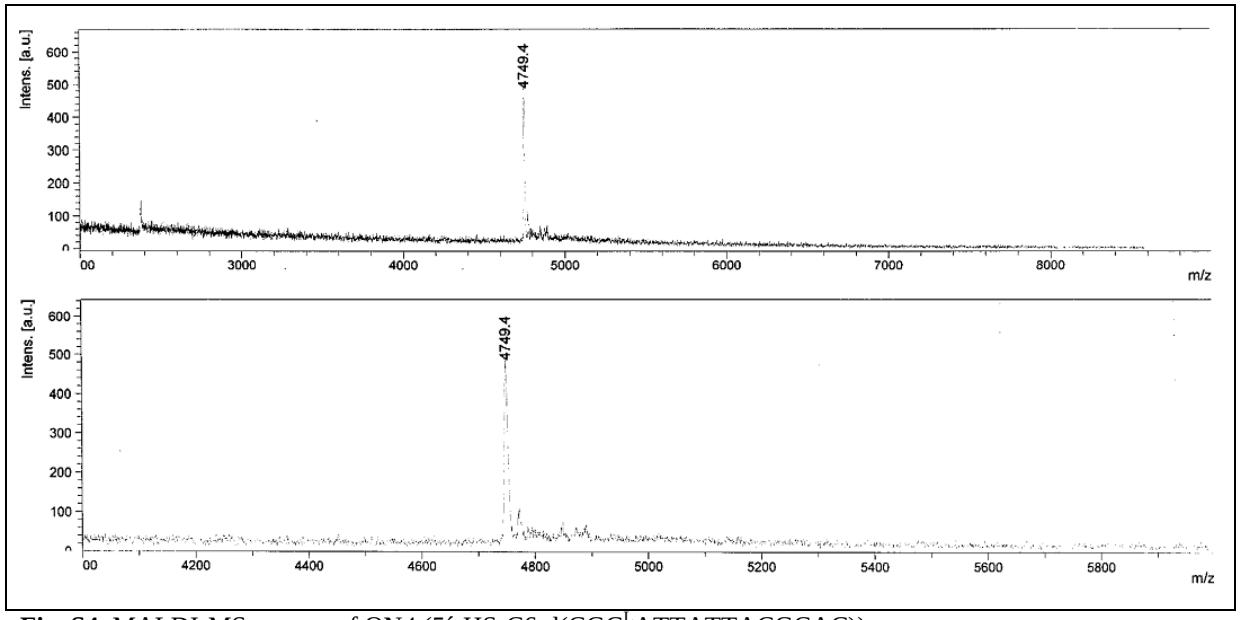

Fig. S4. MALDI-MS spectra of ON4 (5´-HS-C6-d(CGC^{L}ATTATTACGCAC)).

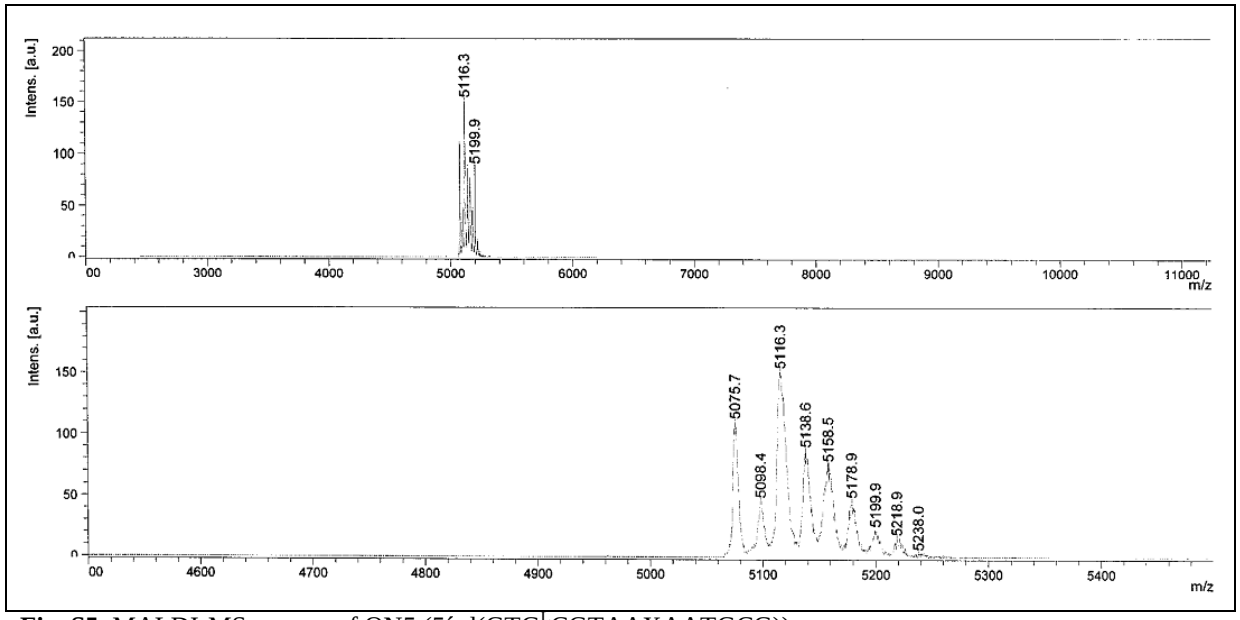

Fig. S5. MALDI-MS spectra of ON5 (5´-d(GTG^{L}CGTAAXAATGCG)).

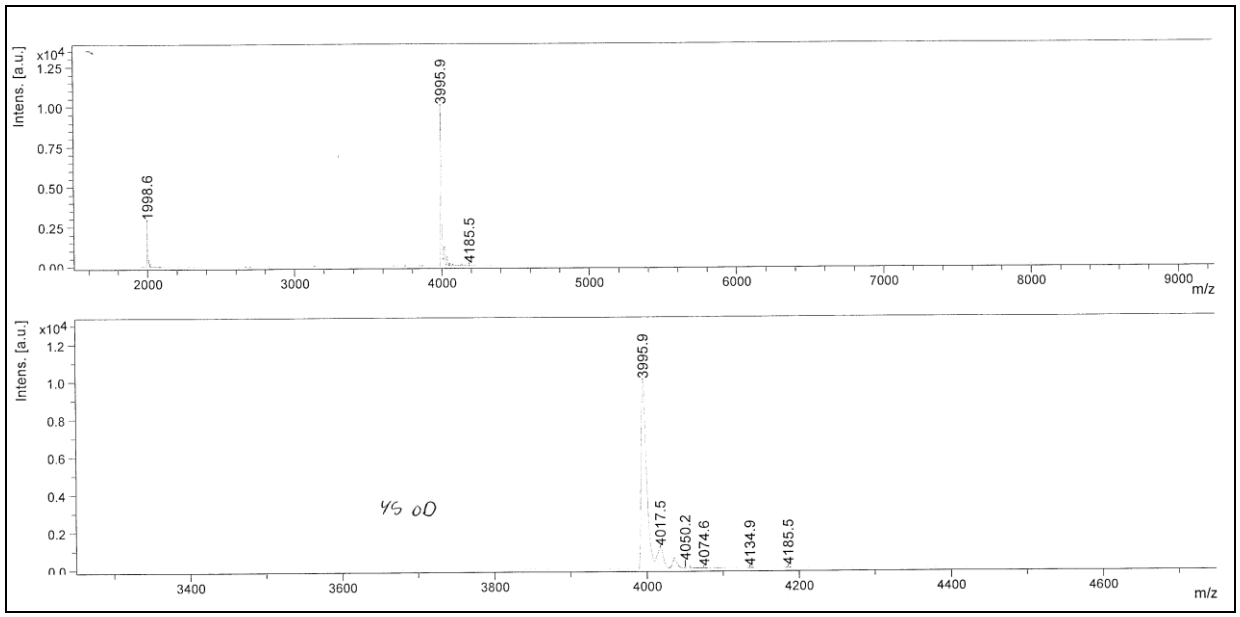

Fig. S6. MALDI-MS spectra of ON6 (5´-d(GCGTAATAATGCG)).

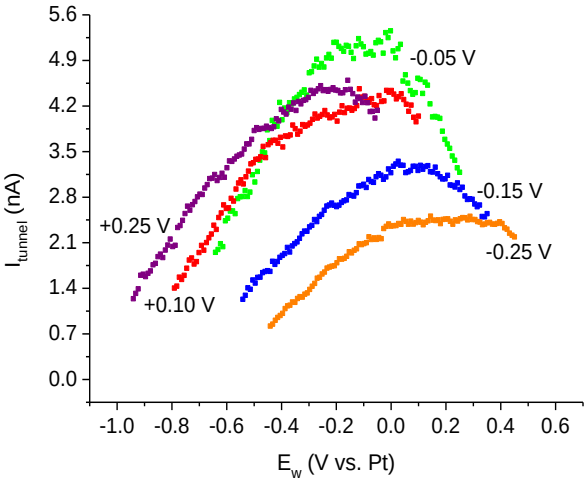

Fig. S7. Tunnelling current/overpotential correlations for terpy-free15-base ss-DNA (ON4) functionalized by $RuCl_3$ on a Au(111)-electrode surface in 10 mM KH_2PO_4/K_2HPO_4 (pH 7.0). The bias voltages are indicated. The modulus of the negative current values was taken for the negative bias voltages to aid presentation of the STS-spectra side-by-side. Scan rate 0.6 V s^{-1}.

S.2 Ionic Strength Dependence of the STS Bandwidth

The *in situ* STS peak width depends primarily on the potential distribution in the tunnelling gap, in turn determined by the ionic strength[47,67-69]. Two parameters are crucial, viz. the fraction of the potential drop from the working electrode surface at the site of the redox centre, ξ and the fraction of the bias voltage drop at this same site, γ. In crude terms $\xi = 1$ corresponds to the full potential drop as common at semi-infinite electrode surfaces but the distribution is more composite in the tunneling gap of widths, L comparable to the Debye length, L_d of the electrolyte. L_d varies from ≈ 1 nm at electrolyte concentrations around 0.1 M to ≈ 3 nm at 0.01 M. The tunnelling gap width L cannot be determined precisely but is comparable to the "size" of the molecules. The latter depends on the molecular conformation but values around 3 nm are likely. Presently we note that within the Debye approximation ξ and γ are correlated[47,67-69]

$$\xi(z;L_d) = 1-\gamma(L-z;L_d)-\gamma(z;L_d)\ ; \qquad \gamma(z;L_d) = \frac{\exp\left(\frac{z}{L_d}\right)-\exp\left(-\frac{z}{L_d}\right)}{\exp\left(\frac{L}{L_d}\right)-\exp\left(-\frac{L}{L_d}\right)}$$

(S1)

where z is the position of the redox group counted from the substrate electrode surface. The width at half height of the tunneling peak, Δ_η [47,67-69] is

$$\frac{\Delta_\eta}{k_B T} = \frac{4arch(2)}{1-\gamma(L-z;L_d)-\gamma(z;L_d)} \qquad \text{(S2)}$$

The following is then notable:

- At high ionic strength $L_d << L$. For a symmetric location of the redox centre, z = ½, and eqs.(1) and (2) reduce to

$$\gamma^{high.ion}(\frac{1}{2}L;L_d << L) \approx exp\left(-\frac{1}{2}\frac{L}{L_d}\right) << 1\ ; \qquad \frac{\Delta_\eta^{high.ion}}{k_B T} \approx 4arch(2) = 5.2 \qquad \text{(S3)}$$

while low ionic strength gives

$$\gamma^{low.ion}(\frac{1}{2}L;L_d \approx L) \approx \frac{1}{e^{\frac{1}{2}}+e^{-\frac{1}{2}}} = 0.443\ ; \qquad \frac{\Delta_\eta^{low.ion}}{k_B T} \approx \frac{4arch(2)\left(e^{\frac{1}{2}}+e^{-\frac{1}{2}}\right)}{e^{\frac{1}{2}}+e^{-\frac{1}{2}}-2} \qquad \text{(S4)}$$

- Δ_η thus increases significantly, from $\Delta_\eta \approx 5.2 \times k_B T \approx 0.13$ eV to about $\approx 46 \times k_B T \approx 1.16$ eV when the ionic strength is lowered from high values, say 0.1-1 M to low values, say < 0.01 M for z = ½. The width also rises drastically when the redox group is located close to either of the enclosing electrode surfaces.
- γ is small, i.e. close to zero at high ionic strength but close to ½ at low ionic strength for symmetric location of the redox group. Significantly larger values arise when the redox group is close to either of the enclosing electrode surfaces.